Singular Wire-Driven Series Elastic Actuation with Force Control for a Waist Assistive Exoskeleton, H-WEXv2

Dong Jin Hyun, HyunSeop Lim, SangIn Park, and Seungkyu Nam

***Abstract*—This article presents a design of an electrically powered waist-assistive exoskeleton H-WEXv2 to reduce back-muscle fatigue and prevent back-injury of industrial workers. It utilizes a wire-driven mechanism based on a singular series elastic actuation to achieve system performances in aspect of cost, weight, operational time, and system endurance and maintainability for industrial feasibility. This proposed mechanism consisting of a ball screw drive and a series elastic actuator enables H-WEXv2 to accomplish better control maneuverability on powered flexion/extension while maintaining the advantage of allowing natural human walking with almost zero impedance. Also, to transfer torque determined by a high-level controller, a *SEA force controller* was implemented by measuring elastic displacements of installed spring elements at both hip joints. In order to evaluate the effectiveness of the developed robot installed with the proposed mechanism, electromyographic (EMG) signals of relevant muscles of ten subjects related to target waist motions were measured and compared for three cases: 1) wearing H-WEXv1, 2) wearing H-WEXv2, and 3) wearing nothing. Finally, the statistical analysis on acquired EMG signals verified the effectiveness of waist assistance provided by H-WEXv2.**

***Index Terms*—Force control, lower-limb exoskeleton, series elastic actuator, under-actuation, waist assistance.**

I. Introduction

With the social trend of low fertility, aging society, and the introduction of the concept of smart factory, exoskeleton technologies have started to be considered as a potent solution in medical [1] and industrial [2] applications. Incidents of back disorders are statistically reported to be higher, especially for workers who are consistently exposed to repetitive lifting, bending, and twisting of the back. In the areas of construction, farming, transportation, storage, human health, and social work, individuals are required to do such tasks for fairly long periods of time. Because of these working environments, musculoskeletal diseases, including back disorder, were reported to be emerging worldwide [3], [4]. The back-pain associated medical expenses and loss of productivity are estimated to produce a socioeconomic loss over $100 billion in the U.S. alone [5].

For the prevention of back-injury or back-pain, various passive/active types of assistive exoskeletons have been developed and applied to real industrial environments with promising results. It is said that up to 40% reduction in back muscle activity could be achievable while utilizing a waist assistive exoskeleton [6]. Furthermore, it was reported that on-body devices such as exoskeletons could be more acceptable to workers as a viable means, even though off-body aid devices such as fork-lifts and hoists can be utilized for the same purpose in the industrial environment [7].

Taking inherent advantage of lightweight passive devices, various energy-restoring mechanisms have been proposed and assessed for prevention of back-injury [8]–[10]. Passive commercial exoskeletons, such as the BackX[1](weight: 3.3 kg) and the Laevo[2] (weight: 2.8 kg) received recognition due to an appropriate tradeoff between weight and assistive forces. However, these assistive devices have definite limits in terms of versatility due to the inability of modulating the assistive forces provided. Thus, active waist assistive exoskeletons have been released to the market with competitive weights and maximum assistive forces; for example, ATOUN MODEL Y[3] [11] weighs 4.8 kg providing the maximum assistive force of 10 kgf, and HAL Lumbar Support [12] is known to weigh just 3 kg with an unspecified maximum assistive force.[4] Fig. 1 shows the comparison chart for several powered waist assistive exoskeletons, including H-WEXv2 presented in this article. It represents the positioning of various active robots in terms of maximum assistive force and weight in the form of a chart. The maximum assistive force can be defined as the maximum force exerted on the torso using a harness which is attached to a mechanical frame. Type and number of actuators are also indicated in Fig. 1. Different from other exoskeletons, both H-WEXv1 and v2 utilize singular actuation providing competitive light-weight and affordability without

Manuscript received February 11, 2019; revised July 11, 2019, September 23, 2019, and December 12, 2019; accepted January 25, 2020. Date of publication January 30, 2020; date of current version April 15, 2020. Recommended by Technical Editor C.-C. Lan. *(Corresponding author: Dong Jin Hyun.)*

The authors are with the Robotics Lab in the R&D Division of Hyundai Motor Company, Uiwang-si 16082, South Korea (e-mail: mecjin@gmail.com; hyunseop@hyundai.com; ppaksang@gmail.com; seungkyu83@gmail.com).

Color versions of one or more of the figures in this article are available online at https://ieeexplore.ieee.org.

Digital Object Identifier 10.1109/TMECH.2020.2970448

[1][Online]. Available: https://www.suitx.com/backx

[2][Online]. Available: http://www.laevo.nl/

[3][Online]. Available: http://atoun.co.jp/products/atoun-model-y

[4][Online]. Available: https://www.cyberdyne.jp/english/products/Lumbar_LaborSupport.html

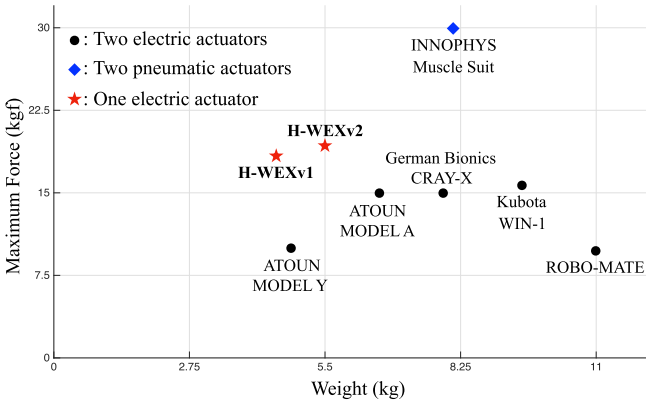

Fig. 1. Comparison chart for maximum assistive forces with respect of weights of several back-support exoskeletons (all values are available in the website for each product except for ROBO-MATE [13]. Its maximum assistive force is estimated from its maximum assistive torque when its length of the moment arm is 0.42 m, which is same for H-WEXv2.).

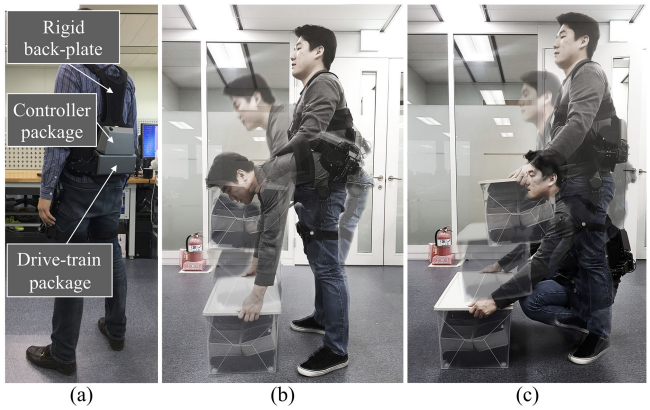

Fig. 2. (a) Wearing photo with H-WEXv2, and overlapped photos describing its two target assisted waist motions, (b) in stooping postures, and (c) in crouching postures.

losing the capability of generating high force. Passive waist exoskeletons are not considered in the chart because they must be evaluated in different aspects from active exoskeletons. For example, increase in stiffness of a spring element for a passive exoskeleton with regardless of its usability performance can lead to increase in maximum force without much increase in weight. Recently, MK2 utilized two parallel elastic actuators to relax the maximum torque requirement by means of elastic elements [14]. This parallel active/passive mechanism is intended to occupy a more advantageous position in a tradeoff between weight and assistive forces. Therefore, passive/active or hybrid powered exoskeletons might each reveal advantageous performance in terms of the selected tradeoff depending on target motions to be assisted. We expected research on waist assistive exoskeletons to be continuously conducted to develop robots heading toward the upper left direction of the chart in Fig. 1 while removing discomfort due to weight and overcoming insufficient torque transmission.

In this article, we introduce the Hyundai Waist Assistive Exoskeleton version II (H-WEXv2) with a series elastic actuating wire-driven mechanism, which results in the improvement of its performance while maintaining advantages previously achieved by H-WEXv1 [15]. In both versions, this single-actuator power-transmission approach differs from other waist-assistive devices of the same type that utilize two actuators at both hip joints [16]–[18]. Through this reduction in the number of actuators as in H-WEXv1, it was anticipated that a low cost, lightweight, and power-saving solution for waist assistance using simple electrical wiring could be effectively achieved. Also, it allowed both hip joints to move with minimal mechanical impedance in each opposite direction for normal walking.

However, the differential mechanism of H-WEXv1 had an inherent limitation, as it was only able to transmit one way force in the direction of the waist extension. This solution led to a problem associated with wire slackness, which made the user experience worse. Also, using this solution to support crouching postures [see Fig. 2(c)] required a relatively complex high-level controller. As a result, H-WEXv1 solely discriminated and assisted stooping postures accompanied with upper body movements. In order to overcome these limitations, a wire-driven ball-screw drive mechanism was applied for HWEXv2 shown as a wearing photo in Fig. 2(a). This proposed mechanism is more affordable compared to the previously utilized differential mechanism, and it allows bidirectional power transmission. Moreover, it is able to perform delicate force control with a method of series elastic actuation (SEA) [19]. Thanks to these advantages provided by H-WEXv2, the target assistive motions are able to include not only motions at stooping postures in Fig. 2(b), but also motions at crouching postures in Fig. 2(c), utilizing a simple high-level controller explained in Section III.

TABLE I
MECHANICAL SPECIFICATION FOR THE DEVELOPED H-WEXv2

Description	Value
weight (kg)	5.5 including batteries
size (mm)	450 ∼ 500 (W)×560 (H)×220 ∼ 230 (D)
Max. assist torque (Nm)	94.5
Max. hip joint angular velocity (deg/s)	689
Operational voltage (V)	40
Gear ratio (G)	34.38 : 1

The rest of this article is structured as follows. Section II introduces the mechanical design of H-WEXv2 including the wire-driven SEA and its low-level indirect force controller. Section III explains the high-level controller for waist assistance. Subsequently, experimental procedures and evaluation data are provided in Section IV. Finally, Section V concludes this article.

II. MECHANICAL DESIGN OF H-WEXv2

A. Overall Mechanical Design

Overall specification of the mechanical structure of H-WEXv2 is briefly noted in Table I. It has a total of six degrees of freedom (DoFs) consisting of two bidirectional under-actuated DoFs for hip flexion/extension, two passive DoFs for abduction/adduction of each leg, and further two passive DoFs for each thigh cuff. These last DoFs were intended to allow the thigh cuff to freely rotate in the roll direction to adapt to the wearer's thigh shape. In this way, wearing discomfort can be reduced. A pilot product of H-WEXv2 was developed to

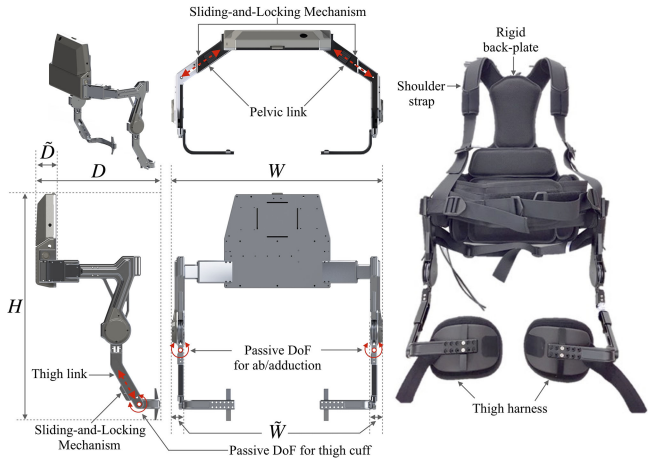

Fig. 3. Mechanical structure of H-WEXv2.

acquire feedback from the wearers, so that the device can be made adjustable with various body shapes. In order to cater for variations in human trunks, the width (W) and the depth (D) in Fig. 3 are designed to be simultaneously length-adjustable through a sliding-and-locking mechanism installed in the pelvic link. When adjusting the link-length, the ratio of length variation of W with respect to length variation of D is set to be 1.34 referring to human body measurement data.[5]

Also, a similar mechanism is also applied to the thigh link to cover size variants of thighs if necessary. These length-adjustable mechanisms can cause an increase in the total weight of the robot. Therefore, if the link-lengths of the robot can be initially customized only for one person, these mechanisms are unnecessary and can be removed such that the robot's weight can be reduced. Therefore, the mechanisms are planned to be removed or replaced by another light-weight mechanism after the model-fixing process.

Basically, the robot is wire driven by a singular actuator consisting of a 100 W brushless direct current (BLDC) motor (Maxon EC-i 40 operated nominally by a 36 V power source) and a ball-screw drive system (5 mm/rev pitch). For better durability, the material for the wire was carefully selected to be Dyneema's tear-resistant drive rope (3800 N).[6] The torque/velocity specification for the actuation system was determined referring to kinetic/kinematic analysis based on a biomechanical model [20]; it aims at maximally providing approximate half of the full necessary waist torque. This proposed actuation system enabled low-cost implementation due to the removal of previously utilized harmonic drive (generally expensive) and allowed really small values for both thicknesses of the backpack ($\tilde{D} = 52$ mm) and the hip joint ($\tilde{W} = 32$ mm). These are crucial design parameters related to usability of wearers in various environments. Also, the back plate was designed to be short such that it does not approach the neck of a wearer because of the past experiences with H-WEXv1.

[5][Online]. Available: https://sizekorea.kr/

[6][Online]. Available: https://www.dsm.com/products/dyneema/en_GB/applications/ropes-lines-and-slings.html

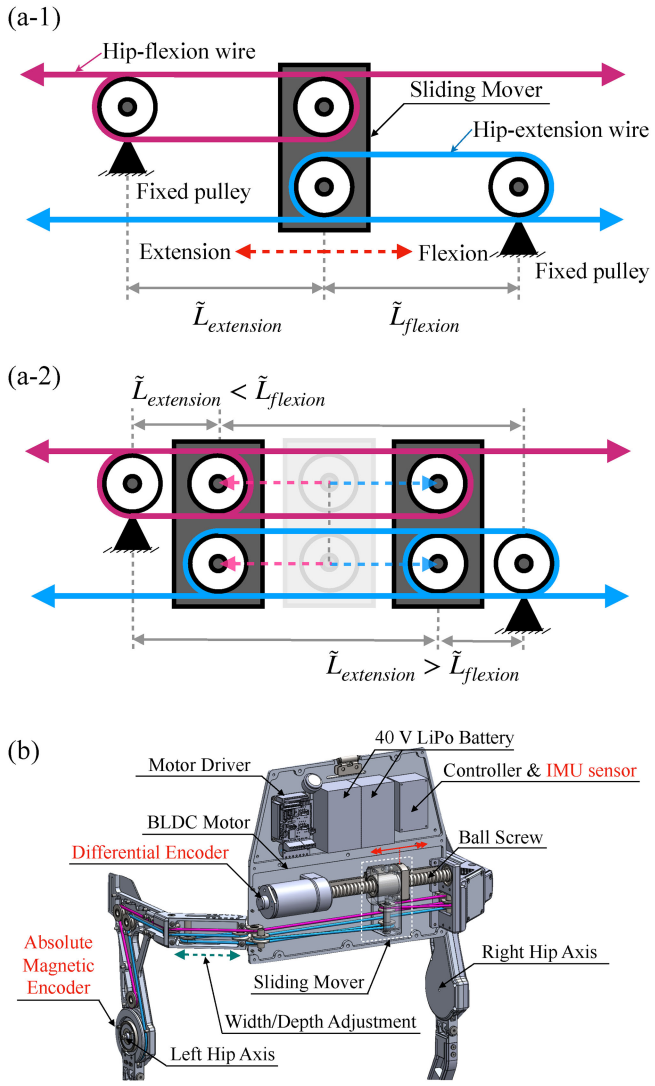

Fig. 4. Configuration of singular wire-driven actuation based on a ball-screw drive system; (a-1) conceptual drawing describing principles of both powered hip flexion/extension, (a-2) operation examples: the sliding mover moves leftward for powered hip flexion ($\tilde{L}_{\text{extension}} > \tilde{L}_{\text{flexion}}$) and moves rightward for powered hip extension ($\tilde{L}_{\text{extension}} < \tilde{L}_{\text{flexion}}$), (b) implementation of the proposed mechanism on the developed H-WEXv2; sensors are indicated by red letters.

Previously, H-WEXv1 provided a stiff long back plate, which interfered with natural waist movement of a wearer. Instead of the stiff long back-plate, we replaced that part with a short rigid plate harness connecting the top of the robot to a wearer's shoulder.

B. Principle of Proposed Wire-Driven Power-Transmission for Back Support

The wire-driven mechanism for power transmission of H-WEXv2 is conceptually described in Fig. 4(a-1). The sliding mover in the middle is horizontally power-actuated along the ball-screw drive system. Each hip-flexion/extension wire is wound around both the corresponding fixed pulley and the corresponding sliding-mover-mounted pulley, then wound wires

extend down to left/right thigh links along the path guided by the pulleys mounted on the structure of H-WEXv2. With this configuration the movement of the sliding mover leads to mutually opposite directional changes in relative distances between the sliding mover and left/right fixed pulleys. These relative distances are indicated as $\tilde{L}_{\text{extension}}$ and $\tilde{L}_{\text{flexion}}$ in Fig. 4. As shown in Fig. 4(a-2), for instance, when powered hip flexion is necessary, the sliding mover is controlled to move leftward, which leads to $\tilde{L}_{\text{extension}} > \tilde{L}_{\text{flexion}}$, and vice versa. The constituted relation on relative distances is expressed in (1) such that the force generated in the actuator is transmitted for the powered hip-flexion by pulling the hip-flexion wire and simultaneously releasing the hip-extension, or vice versa

$$\Delta\tilde{L}_{\text{extension}} = -\Delta\tilde{L}_{\text{flexion}}. \tag{1}$$

Equation (1) can be interpreted such that the robot's left hip-flexion/extension angle (θ_{LH}) is kinematically constrained to the right hip-extension/flexion angle (θ_{RH}) as

$$\theta_{\text{LH}} + \theta_{\text{RH}} = \theta_h. \tag{2}$$

It is noted that with this constraint, the sum of both hip angles (θ_h) can be controlled by the proposed singular actuation system with the SEA mechanism. In this article, the average value of both hip angles, i.e., $\frac{\theta_h}{2}$, is noted as the angle of the virtual thigh segment which is defined in Section III. For normal walking, it has been observed that the direction of motion of each hip joint is opposite to that of the other except during a specific gait phase known as double stance [21]. Therefore, under the constraint (i.e., almost fixed θ_h), both hip joints can be mutually moved in the opposite direction with minimal impedance while walking with normal gaits. When assistive torque is necessary to lift-up his or her torso, the singular actuator is controlled to generate torque in the direction such that θ_h can be decreased.

Especially, the powered both hip-flexion (i.e., waist-flexion) is allowed with this mechanism, but was not allowed with the H-WEXv1 due to the limitation of one-way power-transmission based on a differential gear. This improvement can be utilized for control action to prevent overextension of both hips which often causes discomfort at the end of assistive hip-extension.

For the implementation of the proposed mechanism, each component of the actuation system including a motor driver, 40 V LiPo battery is deployed as Fig. 4(b). For building up feedback control with a customized embedded controller (180 MHz ARM Cortex-M4F), the absolute magnetic encoder to measure angles of hip-flexion/extension is mounted on the hip joint, and an inertial measurement unit sensor is installed on the back part to estimate orientation of a wearer's torso. Also, the position of the sliding mover is calculated through the differential encoder on the BLDC motor. To calibrate the neutral position of the sliding mover, the absolute encoders mounted on both hip joints are utilized when a wearer initially uses H-WEXv2 in a neutral standing posture without any interactive force.

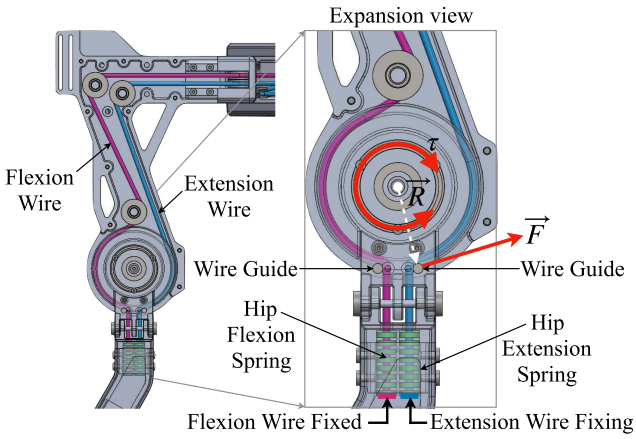

Fig. 5. Description of wire-driven serial elastic actuation.

C. SEA Mechanism With Low-Level Controller for Indirect Force Control

The hip flexion/extension wires are extended to the thigh part and fixed together with an elastic component to constitute SEA for force control as shown in Fig. 5. The spring stiffness constant, k_s, for the installed spring element was decided to be the value of 36.25 N/mm. The spring element was selected to have a typical size, so it can be easily replaceable to have more stiff elasticity for avoiding the limited force control bandwidth which is the representative drawback of SEA. While implementing the design of a controller, the spring elements of the SEA were replaced two times to achieve sufficient control bandwidth required for waist motions. With this SEA structure, tension force, F, exerted on each wire deforms the corresponding spring displacement ΔX by Hooke's law in (3)

$$\Delta X = \frac{F}{k_s}. \tag{3}$$

Assuming this static force relation can describe interactive force being transmitted to human body, force control can be executed by regulating the total summed deformation of hip-flexion spring (ΔX_{flex}) and hip-extension spring (ΔX_{ext}), which have the relation of (3) with tension forces on each wire. This total deformation ΔX is easily calculated by utilizing both the absolute magnetic encoder on the hip joint and the differential encoder on the BLDC motor. In other words, the angular displacement by being wire-pulled or wire-pushed in the BLDC motor side is different from the actual average angular displacement for both hip joints by ΔX, which enables the estimation of the flexion/extension tension force on each wire. The direction of the regulated tension force is changed through the wire guide in Fig. 5; as a result, the reaction force $\vec{F}$ on the wire guide leads to the exerted torque on the hip joint $\vec{\tau} = \vec{R} \times \vec{F}$ where $\vec{R}$ in Fig. 5 is the vector of which magnitude is the radius of the hip pulley (33.5 mm). Consequently, 13% of the tension force results in loss because it has a component parallel to the direction of $\vec{R}$ due to the kinematic position of the wire guide, but this is not avoidable for the installation of the elastic element of SEA. Therefore, the

TABLE II
CONTROL PARAMETERS FOR SEA FORCE CONTROL AND MAXIMUM DEFORMATION LENGTH FOR INSTALLED SPRING ELEMENTS

Description	Value
K_p	1
K_d	0.01
ΔX_{max}	smaller than 38 mm

magnitude relation between $\vec{F}$ and $\vec{\tau}$ can be described as

$$|\vec{\tau}| = \eta |\vec{R}||\vec{F}| = \frac{1}{\xi}|\vec{F}| \tag{4}$$

where $\eta = 0.87$ is the force transfer rate. The effective transmission ratio ξ is calculated to be 34.311 m^{-1}.

A low-level controller was developed to regulate the exerted force to follow the desired force F_d by SEA force control method [22] as expressed as follows:

$$F = F_d + K_p(F_d - F) + K_d(\dot{F}_d - \dot{F}). \tag{5}$$

Thus, we can convert (5) and (6) to determine the commanded value for the motor current, I_{cur}

$$I_{\text{cur}} = \frac{\left(F_d + K_p(F_d - k_s\Delta X) + K_d(\dot{F}_d - k_s\Delta \dot{X})\right)}{\xi G k_I} \tag{6}$$

where k_I is the torque constant, 74.9 mN/A, for the selected motor, and G in Table I is the gear ratio indicating the relation between torque generated by the motor and torque exerted to both hip joints. When the desired force F_d is determined, the low-level control commands the motor driver to flow I_{cur} in the BLDC motor according to (6). The control parameters for the SEA force control were heuristically tuned in the experiment to have values as shown in Table II and the maximum deformation-length of the installed spring element is slightly smaller than 38 mm, which is the value on its specification sheet due to its mounting length.

III. DESIGN OF SIMPLE HIGH-LEVEL CONTROLLER FOR ASSISTING TARGET MOTIONS

The design of the high-level controller aims at generating effective waist torque for target assist motions in both postures as mentioned earlier, i.e., 1) stooping posture and 2) crouching posture. Basically, in order to assist waist motions with target postures, the high-level controller was designed based on a similar methodology as the previous control scheme implemented on H-WEXv1 [15]. The more advanced, H-WEXv2 has the benefit of providing powered waist flexion/extension for implementing virtual springy constraints without the problem of wire slackness. Therefore, its control algorithm is more simplified due to the removal of the previously used finite state machine (FSM). This FSM consisted of walking and waist assist states, and its use was necessary to discriminate when the drive wire had to be pulled without wire slackness. To accomplish waist assistance and reduce load of the erector spinae as analyzed in [23], the high-level controller is intended to command the lower-level controller to generate a value of motor current corresponding to the determined assistive torque τ_{tot}. This desired torque is the summed value of assistive torques which are resultant from four control actions as shown in (7)

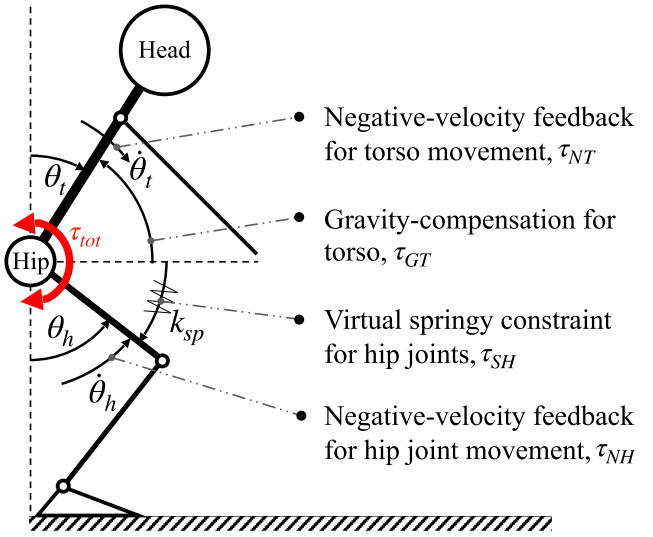

Fig. 6. Description of each control action on the simplified human model.

$$\tau_{\text{tot}} = \tau_{\text{GT}} + \tau_{\text{NT}} + \tau_{\text{SH}} + \tau_{\text{NH}}. \tag{7}$$

With these notations, each control action for each term is explained below, and is also described in Fig. 6.

1) τ_{GT}: Gravity-compensation torque for reduction of gravitational effect on a wearer's torso.
2) τ_{NT}: Negative velocity feedback-control torques with angle-dependent variable gains for angular velocities of a wearer's torso.
3) τ_{NH}: Negative velocity feedback-control torques with angle-dependent variable gains for angular velocities of a virtual thigh segment.
4) τ_{SH}: Required torque to generate a desired springy stiffness according to a virtual constraint on a virtual thigh segment.

In Fig. 6, θ_t represents estimated torso clockwise angular posture with respect to the vertical direction, and $\dot{\theta}_t$ represents θ_t's time derivative. Inherently, H-WEXv2 utilizes the one-DoF powered under-actuation system, so both hip angles are treated to be controlled together based on sensing the angle between the torso and the virtual thigh segment. The virtual thigh segment is defined to be the averaged angular posture for both thigh links with respect to the vertical direction as expressed in (8), where θ_h is an averaged value for both hip-joint counter-clockwise angular postures with respect to the vertical direction, i.e., θ_{RH} or θ_{LH}

$$\theta_h = \frac{\theta_{\text{RH}} + \theta_{\text{LH}}}{2} \tag{8}$$

and $\dot{\theta}_h$ stands for its time-derivative value. Finally, k_{sp} is the value of programmable virtual stiffness on the virtual thigh segment.

Each value of resultant torques given from control actions is mathematically expressed as follows:

$$\tau_{\mathrm{GT}} = \begin{cases} G_{\mathrm{ratio}} L_{\mathrm{tot}} m_{\mathrm{tot}} g \sin\theta_t, & \text{if } \theta_t > 0 \\ L_{\mathrm{tot}} m_{\mathrm{tot}} g \sin\theta_t & \text{otherwise} \end{cases}.$$

$$\tau_{\mathrm{NT}} = \begin{cases} k_{\mathrm{td}} \tilde{f}_{\mathrm{tv}} \dot{\theta}_t, & \text{if } \dot{\theta}_t < 0 \\ 0, & \text{otherwise} \end{cases}$$

$$\tau_{\mathrm{SH}} = G_{\mathrm{ratio}} k_{\mathrm{sp}} \theta_h$$

$$\tau_{\mathrm{NH}} = \begin{cases} k_{\mathrm{hd}} \tilde{f}_{\mathrm{hv}} \dot{\theta}_h, & \text{if } \dot{\theta}_h < 0 \\ 0, & \text{otherwise} \end{cases}. \tag{9}$$

In these equations, L_{tot}, m_{tot}, g are the distance between the hip joint and the center of mass (CoM) of a wearer's torso, torso mass, and the gravity constant. In an actual implementation, m_{tot} can be chosen to be a control variable indicating the torso mass to be assisted. For experiments in Section IV, m_{tot} was set to be 10 kg. There are no discontinuities in these switching actions in (9) because two functions in the case-structure corresponding to each torque are mutually continuous with respect to its input. For instance, even though it is likely that τ_{GT} seems to have discontinuity at $\theta_t = 0$, both cases actually have zero output at $\theta_t = 0$ regardless of G_{ratio}. Therefore, a specific switching treatment for continuity is unnecessary. Both k_{td} (or k_{hd}) and $\tilde{f}_{\mathrm{tv}}$ (or $\tilde{f}_{\mathrm{hv}}$) for the negative velocity-feedback controls are the constant feedback gains and its torso angle-dependent modulation factors, respectively

$$\tilde{f}_{\mathrm{tv\ or\ hv}} = \begin{cases} 1, & \text{if } \theta_t > \frac{\pi}{4} \\ \sin(2\theta_t) \text{ or } \sin(2\theta_h), & \text{otherwise.} \end{cases} \tag{10}$$

These angle-dependent modulation factors are intended to attenuate τ_{NT} and τ_{NH} when a wearer's posture approaches to have his/her waist fully extended. These also lead to the directional inverse of assistive torque in the angle range of overextension. Therefore, a wearer's feeling of being held back by overextension can be prevented. Also, while having normal walking, noise-actuations due to negative feedback actions can disappear due to their attenuation effect.

Similarly, the gravity compensation torque τ_{GT} and the virtual springy constraint torque τ_{SH} are generated with multiplication of G_{ratio}. H-WEXv2 has a control interface through which a user adjust the value of G_{ratio}. A user can simultaneously adjust the strengths of both gravity compensation and the virtual springy constraint by selecting the value of $G_{\mathrm{ratio}} \in [0.1, 1]$. Especially, when the torso is overextended, τ_{GT} plays a role to return his or her torso to the vertical direction due to negative values of θ_t. This additional advantage given from the enabled powered-flexion is also utilized to prevent overextension by providing a wearer with a feeling of support from behind. This is one of the key improvements on H-WEXv2. Assuming that natural human motion could be generated by joint torques under a bandwidth of 5 Hz [24], the low-pass filter for removal of noises in derivative values for sensor signals is selected to be the second-order 5 Hz-bandwidth butterworth filter.

IV. Experimental Verification on H-WEXv2

A. Operation Experiment

The operational performance was first evaluated based on acquisition of sensor values for 10 s while wearing H-WEXv2. Approximately three repeated waist motions were tested with both stooping and crouching postures. Fig. 7 from top to bottom contains captured plots showing motions of a wearer's torso, its corresponding assistive torque determined by the high-level controller, and motions of the virtual thigh segment. Before acquiring sensor values, the parameter G_{ratio} in (9) was set to be one for evaluation, and the maximum value for exerted torque was limited to be 100 Nm for safety. Pitch angles/velocities of torso/virtual thigh segment describes characteristics of each posture (for the case of taking stooping posture main movements appeared in the torso, and for crouching posture main movements occurred in the virtual thigh segment).

Assuming that Hooke's law in (3) is effective in the installed spring elements and interactive force can be described by this tension force relation, both of the 4th row plots in each column of Fig. 7 indicate the intended force tracking performance of SEA. It was observed that the actual spring-deformation displacement X_a could track the desired displacement X_d inside of the range of approximately 38 mm, but when outside of the range, tracking performance was significantly deteriorated. That is, the maximum spring-deformation length ΔX_{max} in Table II was indicated to be insufficient to cover desired force control range. Thus, when the deformation length is over the range, the SEA force control scheme in (5) plays a degraded force regulation role as

$$I_{\mathrm{cur}} \approx \frac{\left(F_d + K_p(F_d - k_s \Delta X_{\mathrm{max}}) + K_d \dot{F}_d\right)}{\xi G k_I}. \tag{11}$$

In the two-third row plots in Fig. 7, the commanded torque, τ_{tot}, computed by (7) was observed to be saturated due to the set value of the saturation limit (100 Nm). For better large force tracking performance, the spring element is needed to be replaced with one having larger stroke length. Nevertheless, according to a qualitative test of wearers, small force tracking performance of SEA was evaluated to provide better maneuverability with fast and smooth force response than H-WEXv1 as already studied in [25] and [26], and also the degraded large force regulation was not felt to induce problematic discomfort.

B. Assessment of H-WEXv2 Performance Based on Surface EMG Measurements

To figure out assistive effects of H-WEXv2 on body-loading associated with waist motions, we conducted experimental evaluation based on acquired electromyography (EMG) signals related to muscle activities, and we compared each waist assist performance based on measured EMG signals in three cases: 1) wearing H-WEXv1, 2) wearing H-WEXv2, and 3) wearing nothing.

1) EMG Experiment: Ten healthy male subjects [age: 34.9 ± 2.13 years old, height: 176.7 ± 4.76 cm, weight: 73.2 ± 7.52 kg (mean±S.D.)] participated in this experiment. This

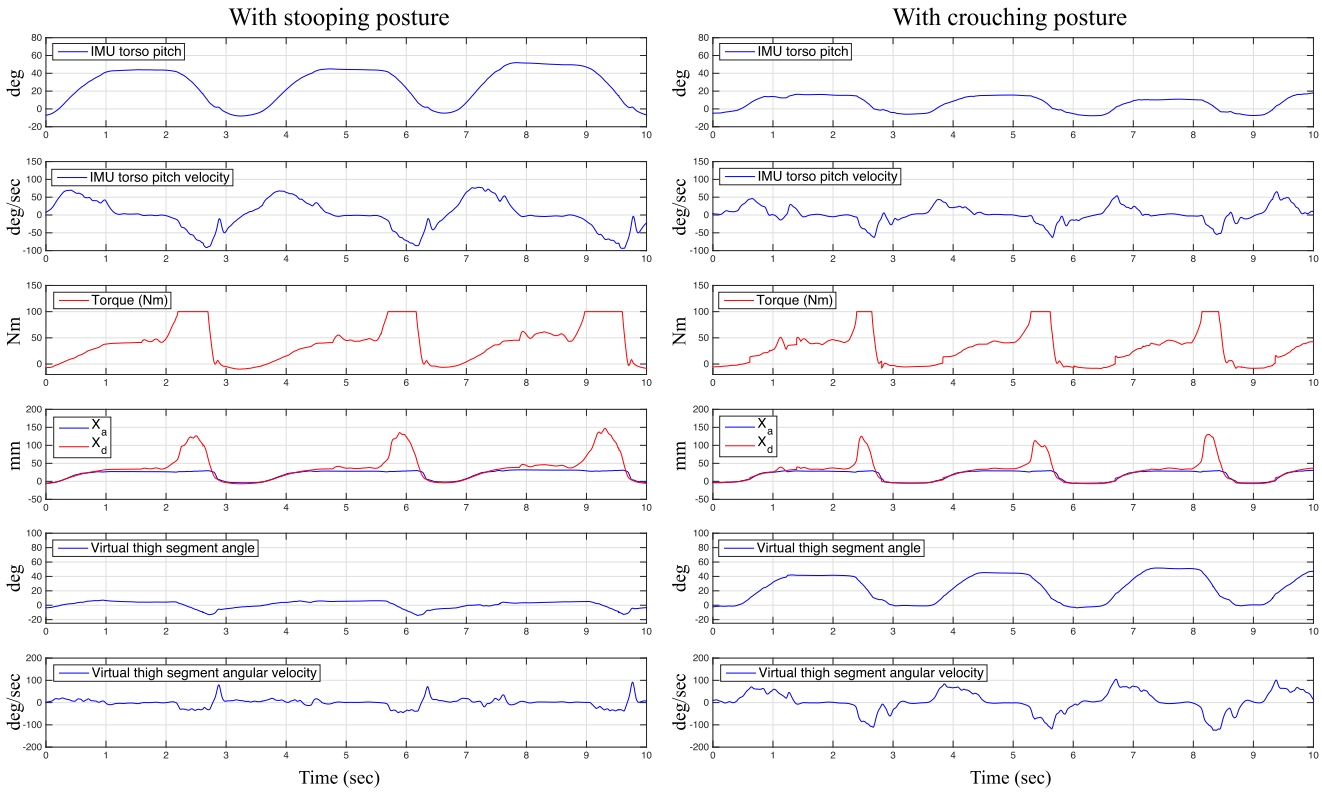

Fig. 7. Experimental results consisting of two multi-plot columns: the first/second column indicates data while repeatedly having waist motion with stooping/crouching posture. each column contains torso pitch (θ_t), torso velocity ($\dot{\theta}_t$), commanded torque (τ_{tot}) computed by (7) and saturated at 100 Nm, actual/desired spring displacement (X_a and X_d) without considering saturation, and the angle of the virtual thigh segment (θ_h) and its velocity ($\dot{\theta}_h$) in order from top to bottom.

EMG-based experiment consisted of evaluations on six conditional waist loading tasks including two motions (stooping posture and semisquatting posture) and three wearing conditions (with H-WEXv1, H-WEXv2, and without H-WEX). The crouching posture, one of the target motions to be assisted by H-WEXv2, was replaced by the semisquatting posture due to the structural limitation of H-WEXv1, which can not allow for convenient crouching postures. Each task involved lifting and lowering a load of 15 kg from knee height to pelvic height. The lifting and lowering trial was consistently repeated five times in each task. The experimental task motion was performed in a similar manner as done previously with H-WEXv1 [15].

EMG signals were measured from five muscles at each side which are rectus abdomins, erector spinae, gluteus maximus, rectus femoris, and biceps femoris as indicated in Fig. 8. These muscles have been known to be mainly related to waist motions. At the end of the all tasks, maximum voluntary contraction (MVC) was measured twice per each muscle [27], [28]. There were sufficient break times between all waist motion tasks and MVC measurement session to reduce unintended effects due to the muscle fatigue and interference.

2) EMG Acquisition and Processing: The EMG data from each muscle was acquired using Delsys Trigno Wireless EMG System (Delsys, Inc., USA). Its data-acquisition sampling rate

Fig. 8. Experiment to acquire surface EMG measurements on motions with two postures: lifting-up a load of 15 kg with (a) stooping posture and (b) semi-squatting posture.

of collected EMG singals was 2000 Hz. Data preprocessing was performed using custom software written in MATLAB. The EMG signals were detrended. Then, the signals were passed through a Butterworth fourth-order band-pass filter using a cutoff frequency range from 30 to 350 Hz and 60 Hz notch filter. To remove highly unexpected noise-values from the EMG signals, the outliers were removed. Thereafter, EMG signals contaminated by the electrocardiogram in trunk muscle were filtered using independent component analysis [29]. Then, the

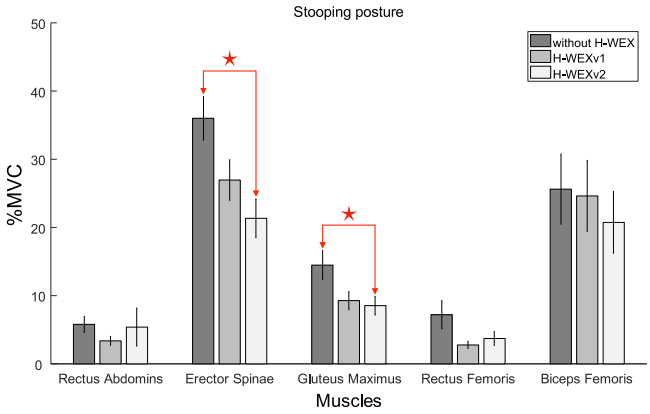

Fig. 9. Statistical result (mean±standard error) of surface EMG measurements on lifting-up motions of ten subjects with stooping posture; star-marked arrows indicate significant difference ($p < 0.05$).

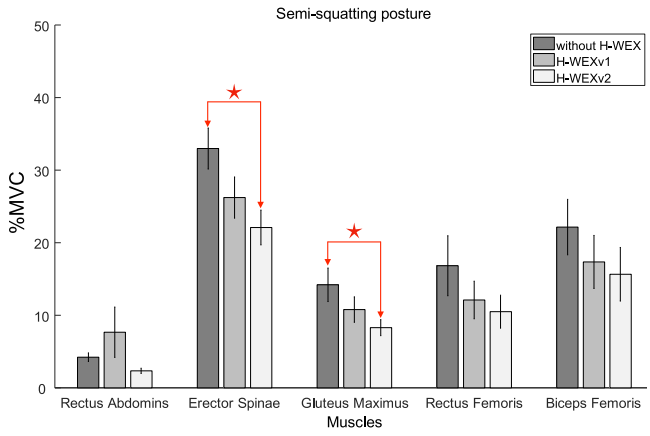

Fig. 10. Statistical result (mean±standard error) of surface EMG measurements on lifting-up motions of ten subjects with semisquatting posture; star-marked arrows indicate significant difference ($p < 0.05$).

RMS of the EMG signal was calculated for the signal intensities, and normalized by the MVC per muscle. The normalized signals were averaged over whole lifting and lowering trials. To compare the EMG intensity of each muscle between three wearing conditions according to the two waist-motions (stooping and semisquatting posture), statistical analysis was performed. Because the EMG data presented a nonnormal distribution ($p < 0.05$; Shapiro–Wilk test), a Kruskal–Wallis ANOVA test was used and Tukey's honestly significant difference (HSD) test was used for post-hoc analysis.

3) Experimental Results: The results of the statistical analyses are shown in Figs. 9 and 10. The muscles activated strongly in the stooping posture were observed to be erector spinae and bicps femoris (see Fig. 9). The semisquatting posture (see Fig. 10), on the other hand, produced an increase in activation of rectus femoris and a decrease in biceps femoris. This indicates that the activated muscle part and its usage varied depending on the postures. Nevertheless, the waist-related muscle was observed to be used the most while taking target motions. Therefore, Erector spinae was the primary muscle in the repetitive task of lifting heavy loads. The results of statistical analyses demonstrated that muscle intensity of erector spinae

Fig. 11. Concept of structural modification on H-WEXv2 for force transmission on torso.

($p = 0.0065, 0.0209$) and gluteus maximus ($p = 0.0447, 0.0366$) in each posture was significantly lower ($p < 0.05$), when the participants were assisted by H-WEXv2 than when not wearing the robot. The muscle intensity of erector spinae and gluteus maximus was reduced by 40.7% and 41.1%, respectively in stooping posture, and 33.0% and 41.6%, respectively in semisquatting posture. The other parts of muscles were observed to show nonsignificant differences between three wearing conditions.

V. Conclusion

This article presents an improved mechanical design concept for an electrically powered waist assistive exoskeleton. The proposed singular wire-driven SEA mechanism is the result of pursuing system performances in terms of cost, weight, operational time, durability, and maintainability of the robot considering requirements for industrial purposes after previously developing the singular wire-driven H-WEXv1. Especially, the proposed mechanism consisting of a ball screw drive and a series elastic actuator enabled us to utilize bidirectional powered waist motions (flexion/extension) with better maneuverability and avoid the use of an expensive harmonic gear. These improvements overcome representative limitations of the previous H-WEXv1. Moreover, it maintains the previously achieved advantages, such as both singular actuated waist assistance and almost zero walking impedance. Therefore, compared to other powered waist assistive exoskeletons, we anticipate that H-WEXv2 could be a better solution in aspects of the requirements mentioned above. In result, this study is expected to help expand the applicability of waist assistive-robots in real-work environments.

According to operational experiments in Section IV-A, it was evaluated that the current spring-element has insufficient stroke-length; therefore, tracking performance was deteriorated at large forces. However, up to 30 Nm, the SEA-based force control could generate forces to track the desired assistive torque. In future work, for better force tracking performance, the installed spring element has to be replaced with one having larger stroke-length or more stiffness without deteriorating force-control bandwidth. Another critical issue is that a

few of the participants in the experiment pointed out that force transmission on their torso through the shoulder strap attached to the rigid back-plate can induce painful discomfort in long-term usage. For the prevention of this unpleasant feeling, the H-WEXv2 link structure for force transmission on torso has to be modified in a way to avoid pulling a wearer's torso by straps by lifting the torso using a chest harness, as shown in Fig. 11. Based on the proposed mechanism with modifications, we further plan to achieve a lighter net weight of the robot by considering application of a novel material and reduce the adjustable-link mechanism through precustomization. Also, we are developing an EMG-based human–robot interface to recognize a wearer's intention that can lead to better performance on usability. Simultaneously, we will conduct an actual field test for the manufacturing, logistics, and nursing fields to continuously improve H-WEX series based on the test data we obtained.

Statistical analysis on the EMG signals acquired from muscles related to waist motions indicated that the H-WEXv2 can effectively reduce the waist muscle activity compared to EMG activations on the case when not wearing the robot. This shows that the assist performance of the proposed mechanism was improved compared to H-WEXv1 as it did not show a significant difference with the case without H-WEX. Further, the EMG reduction achieved by H-WEXv2 was verified to be competitive compared to the EMG test result on other active exoskeletons [30], [31]. Based on these experimental results, we believe that H-WEXv2 can better support prevention of back injuries caused by repeated waist motion in the industrial tasks. It was noted that all of the ten subjects qualitatively evaluated that H-WEXv2 provided comfortable wearability as compared to the previous version, which is due to agile reactive response of the SEA-based force control. Therefore, we conclude that the proposed ball–screw mechanism with bidirectional SEA is verified to provide better performance than the previous harmonic drive based differential mechanism with one-way power transmission.

References

[1] M. Mekki, A. D. Delgado, A. Fry, D. Putrino, and V. Huang, "Robotic rehabilitation and spinal cord injury: A narrative review," *Neurotherapeutics*, vol. 15, no. 3, pp. 604–617, 2018.

[2] R. Bogue, "Exoskeletons–a review of industrial applications," *Ind. Robot, An Int. J.*, vol. 45, no. 5, pp. 585–590, 2018.

[3] C. E. Ekpenyong and U. C. Inyang, "Associations between worker characteristics, workplace factors, and work-related musculoskeletal disorders: A cross-sectional study of male construction workers in nigeria," *Int. J. Occupat. Saf. Ergonom.*, vol. 20, no. 3, pp. 447–462, 2014.

[4] A. Alghadir and S. Anwer, "Prevalence of musculoskeletal pain in construction workers in Saudi Arabia," *Scientific World J.*, vol. 2015, 2015, Art. no. 529873.

[5] S. Dagenais, J. Caro, and S. Haldeman, "A systematic review of low back pain cost of illness studies in the United States and internationally," *Spine J.*, vol. 8, no. 1, pp. 8–20, 2008.

[6] M. P. de Looze, T. Bosch, F. Krause, K. S. Stadler, and L. W. O'Sullivan, "Exoskeletons for industrial application and their potential effects on physical work load," *Ergonomics*, vol. 59, no. 5, pp. 671–681, 2016.

[7] P. Jellema, M. W. van Tulder, M. N. van Poppel, A. L. Nachemson, and L. M. Bouter, "Lumbar supports for prevention and treatment of low back pain: A systematic review within the framework of the cochrane back review group," *Spine*, vol. 26, no. 4, pp. 377–386, 2001.

[8] M. Wehner, D. Rempel, and H. Kazerooni, "Lower extremity exoskeleton reduces back forces in lifting," in *Proc. ASME Dyn. Syst. Control Conf.*, 2009, pp. 49–56.

[9] B. L. Ulrey and F. A. Fathallah, "Subject-specific, whole-body models of the stooped posture with a personal weight transfer device," *J. Electromyography Kinesiol.*, vol. 23, no. 1, pp. 206–215, 2013.

[10] J. Babič *et al.*, "Spexor: Spinal exoskeletal robot for low back pain prevention and vocational reintegration," in *Wearable Robotics: Challenges and Trends*. Berlin, Germany: Springer, 2017, pp. 311–315.

[11] J. Wesslén, *Exoskeleton Exploration: Research, Development, and Applicability of Industrial Exoskeletons in the Automotive Industry*. Jonkoping, Sweden: Jonkoping Univ., 2018.

[12] D. Sasaki and M. Takaiwa, "Development of pneumatic power assist wear to reduce physical burden," in *Proc. IEEE/SICE Int. Symp. Syst. Integration*, 2014, pp. 626–631.

[13] A. S. Koopman *et al.*, "The effect of control strategies for an active back-support exoskeleton on spine loading and kinematics during lifting," *J. Biomech.*, vol. 91, pp. 14–22, 2019.

[14] S. Toxiri, A. Calanca, J. Ortiz, P. Fiorini, and D. G. Caldwell, "A parallel-elastic actuator for a torque-controlled back-support exoskeleton," *IEEE Robot. Autom. Lett.*, vol. 3, no. 1, pp. 492–499, Jan. 2018.

[15] H. K. Ko, S. W. Lee, D. H. Koo, I. Lee, and D. J. Hyun, "Waist-assistive exoskeleton powered by a singular actuation mechanism for prevention of back-injury," *Robot. Auton. Syst.*, vol. 3, no. 1, pp. 492–499, Jan. 2018.

[16] H. Inose *et al.*, "Semi-endoskeleton-type waist assist ab-wear suit equipped with compressive force reduction mechanism," in *Proc. IEEE Int. Conf. Robot. Autom.*, 2017, pp. 6014–6019.

[17] F. Cho, R. Sugimoto, T. Noritsugu, and X. Li, "Improvement of wearable power assist wear for low back support using pneumatic actuator," *IOP Conf. Ser., Mater. Sci. Eng.*, vol. 249, 2017, Art. no. 012004.

[18] H. Yu, I. S. Choi, K.-L. Han, J. Y. Choi, G. Chung, and J. Suh, "Development of a stand-alone powered exoskeleton robot suit in steel manufacturing," *ISIJ Int.*, vol. 55, no. 12, pp. 2609–2617, 2015.

[19] G. A. Pratt and M. M. Williamson, "Series elastic actuators," in *Proc. IEEE Intell. Robots Syst. Human Robot Interact. Cooperative Robots*, 1995, vol. 1., pp. 399–406.

[20] S. Toxiri, J. Ortiz, J. Masood, J. Fernández, L. A. Mateos, and D. G. Caldwell, "A wearable device for reducing spinal loads during lifting tasks: Biomechanics and design concepts," in *Proc. IEEE Robot. Biomimetics Int. Conf.*, 2015, pp. 2295–2300.

[21] E. Ayyappa, "Normal human locomotion, Part 1: Basic concepts and terminology," *JPO: J. Prosthetics Orthotics*, vol. 9, no. 1, pp. 10–17, 1997.

[22] D. W. Robinson, J. E. Pratt, D. J. Paluska, and G. A. Pratt, "Series elastic actuator development for a biomimetic walking robot," in *Proc. IEEE/ASME Int. Conf. Adv. Intell. Mechatronics*, 1999, pp. 561–568.

[23] Z. Luo and Y. Yu, "Wearable stooping-assist device in reducing risk of low back disorders during stooped work," in *Proc. IEEE Mechatronics Autom.Int. Conf.*, 2013, pp. 230–236.

[24] P. R. Cavanagh and P. V. Komi, "Electromechanical delay in human skeletal muscle under concentric and eccentric contractions," *Eur. J. Appl. Physiol. Occupat. Physiol.*, vol. 42, no. 3, pp. 159–163, 1979.

[25] J. F. Veneman, R. Ekkelenkamp, R. Kruidhof, F. C. van der Helm, and H. van der Kooij, "A series elastic-and bowden-cable-based actuation system for use as torque actuator in exoskeleton-type robots," *Int. J. Robot. Res.*, vol. 25, no. 3, pp. 261–281, 2006.

[26] D. Ragonesi, S. Agrawal, W. Sample, and T. Rahman, "Series elastic actuator control of a powered exoskeleton," in *Proc. IEEE Eng. Medicine Biol. Soc., Annu. Int. Conf.*, 2011, pp. 3515–3518.

[27] T. Kim *et al.*, "Electromyographic analysis: Theory and application," *Seoul: Hanmi Med.*, vol. 43, pp. 28–43, 2013.

[28] H. Hislop, D. Avers, and M. Brown, *Daniels and Worthingham's Muscle Testing-E-Book: Techniques of Manual Examination and Performance Testing*. New York, NY, USA: Elsevier Health Sciences, 2013.

[29] N. W. Willigenburg, A. Daffertshofer, I. Kingma, and J. H. van Dieën, "Removing ECG contamination from EMG recordings: A comparison of ica-based and other filtering procedures," *J. Electromyography Kinesiol.*, vol. 22, no. 3, pp. 485–493, 2012.

[30] K. Huysamen, M. de Looze, T. Bosch, J. Ortiz, S. Toxiri, and L. W. O'Sullivan, "Assessment of an active industrial exoskeleton to aid dynamic lifting and lowering manual handling tasks," *Appl. Ergonom.*, vol. 68, pp. 125–131, 2018.

[31] X. Yong, Z. Yan, C. Wang, C. Wang, N. Li, and X. Wu, "Ergonomic mechanical design and assessment of a waist assist exoskeleton for reducing lumbar loads during lifting task," *Micromachines*, vol. 10, no. 7, 2019, Art. no. 463.

Dong Jin Hyun received the B.S. degree in mechanical and aerospace engineering from the School of Mechanical and Aerospace Engineering, Seoul National University, Seoul, South Korea, in 2006, the M.S. degree in mechanical engineering from the University of Michigan, Ann Arbor, MI, USA, in 2007, and the Ph.D. degree in mechanical engineering from the University of California, Berkeley, CA, USA, in 2012.

He was the Postdoctoral Associate with the Mechanical Engineering Department, Massachusetts Institute of Technology, Cambridge, MA, USA in 2013. Since 2014, he has been a Senior Research Engineer with Hyundai Motor Company, Gyeonggi-do, South Korea. His research interests include dynamics and control of legged locomotion, human–robot interaction for wearable robots, and biomechanics.

HyunSeop Lim received the B.S. degree in mechanical and automotive engineering from the Department of Mechanical and Automotive Engineering, Seoul National University of Science and Technology, Seoul, South Korea, in 2009, the M.S. degree in mechanical engineering from the Hanyang University, Seoul, South Korea, in 2011.

He is currently a Senior Research Engineer with Hyundai Motor Company, Gyeonggi-do, South Korea. His research interests include mechanical and actuator design, shape optimization, wearable robots, and biomechanics.

SangIn Park received the B.S. degree in mechanical engineering from the Department of Mechanical Engineering, Hanyang University, Seoul, South Korea, in 2006.

He was with the Korean Branch of National Instruments as an Application Engineer, PAC Specialist and Field Sales Engineer from 2005 to 2013. In 2013, he joined the MIT Biomimetic Robotics Laboratory as a Research Engineer. Since 2014, he has been a Senior Research Engineer with Hyundai Motor Company, Gyeonggi-do, South Korea. His research interests include control architecture design and power electronics.

Seungkyu Nam received the Ph.D. degree in electrical engineering from the Korea Advanced Institute of Science and Technology, Daejeon, South Korea, in 2018.

Since 2018, he has been a Senior Research Engineer with Hyundai Motor Company, Uiwang-si, Gyeonggi-do, South Korea. His research interests include human–computer interaction, machine learning, and bio/brain signal processing.